Development and Demonstration of Large-Aperture Tiled-Grating Compressors for the OMEGA EP Petawatt-Class Laser System

Introduction

The OMEGA EP chirped-pulse–amplification system at LLE requires two 1.5-m large-aperture grating compressors to achieve high-energy petawatt capability.[1] The current state-of-the-art multilayer dielectric (MLD) diffraction gratings cannot meet this size requirement.[2] Several institutes have explored the possibility of tiling gratings.[3–6] Kessler and Cotel have demonstrated the coherent addition of small-scale gold gratings in a compressor using a far-field method.[5,6]

Due to the wavefront of large gratings and the general difficulty in achieving diffraction-limited, far-field performance with a 0.5-m-aperture beam, a far-field method alone cannot provide sufficient tiling accuracy for large-scale grating tiling. We have developed and automated an interferometric tiling method and, for the first time, demonstrated a 1.5-m tiled-grating assembly (TGA) composed of three full-size gratings (0.47 m × 0.43 m, 0.5 m in diagonal).[7] In this article, we report the first demonstration of two large-aperture tiled-grating compressors. The architecture and tiling performance of all eight TGA's developed for the two compressors of OMEGA EP are reported. The tiling technique and the method used for constructing a tiled-grating compressor are described. The full spatial and temporal performance of the tiled-grating compressors is reported.

The following sections (1) describe the pulse compression architecture of OMEGA EP and the development of the tiled-grating assemblies; (2) analyze tiling effect on focal-spot performance and the method for constructing a tiled-grating compressor; (3) present the near-field tiling technique in vacuum and the performance of each tiled TGA; and (4) report on tiling optimization and the characterization of the spatial and temporal performances.

OMEGA EP Pulse-Compression Architecture and Tiled-Grating-Assembly Development

OMEGA EP has two separate grating compressors that produce two short-pulse beams (1 ∼ 100 ps). Figure 115.1(a) shows the pulse-compression scheme for OMEGA EP. Each compressor consists of four sets of TGA's, each having three 0.47-m × 0.43-m gratings. In total, eight TGA's and 24 grating tiles are required to construct the two compressors. The beam size of the OMEGA EP laser is 0.37 m × 0.37 m. The incident angle on TGA1 is 72.5°, which offers a large pulse-compression ratio and relaxes the damage-threshold requirements for the gratings. Figure 115.1(b) shows the rear view of one TGA, which holds three full-size OMEGA EP grating tiles. Each tile is mounted on a triangular support frame. All three tile support frames are mounted on a mechanical platform, with the center support frame fixed to the mechanical platform to provide structural stability. The mechanical platform is positioned on a rotary stage, which allows the entire TGA to rotate between
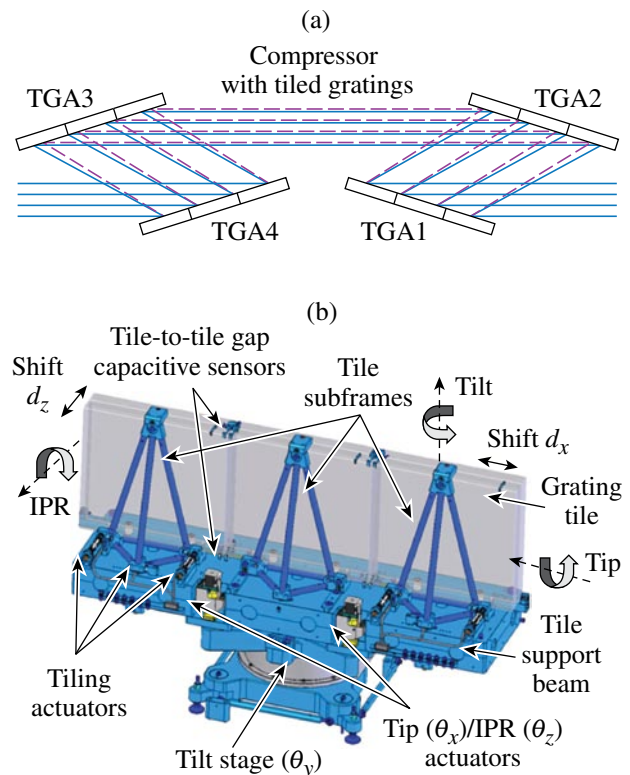
Figure 115.1

(a) OMEGA EP compressor consists of four tiled-grating assemblies (TGA's). The size of each TGA is 1.41 m × 0.43 m. (b) TGA assembly and tiling parameters.

–175° to +175° (θ_y rotation). Tip (θ_x) and in-plane rotation (IPR/ θ_z) movements are provided by two motorized linear actuators mounted on the back of the mechanical platform.

Tile-to-tile alignment is realized by maintaining the central tile static and by moving the two outboard tiles relative to the central tile. For each outboard tile, there are six degrees of freedom relative to the central tile: tilt θ_y, tip θ_x, IPR θ_z, lateral shift d_x, longitudinal shift (also referred to as piston d_z), and relative groove-spacing change Δ_d. The six parameters form three independent pairs: piston and lateral shift, tip and IPR, and tilt and groove spacing change. The two parameters within each pair compensate each other;[8] therefore, each of the outboard tile support frames incorporates only three electrostrictive actuators to provide tile-to-tile alignment by modifying tip, tilt, and piston. Each actuator is paired with a capacitive sensor to form a closed control loop to hold its position. The resolution for holding the position of an actuator is ±4 nm. For coarse alignment, the TGA is positioned at normal and Littrow angles iteratively to remove the tip and IPR of the central tile by adjusting the two linear actuators. The grating grooves of outboard tiles can be aligned to that of the central tile by manually adjusting the tip and IPR through three screws underneath the tile support beam. The initial aligned position is determined by interferometric analysis. The changes from the aligned positions in terms of piston and lateral shift, tip, and IPR are monitored by two pairs of capacitive sensors across the tile gap mounted on the top and bottom surfaces of the tile substrates. The aligned position is then maintained in real time by compensating the temporal drift of the lateral shift and the in-plane rotation with the piston and tip, respectively. Eight sets of TGA's have been built for the two compressors of OMEGA EP.

Modeling for Focal-Spot Analysis and Tiled-Compressor Construction

A ray-tracing model has been developed to perform tiling tolerance analysis for the full tiled-grating compressor system followed by an *f*/2 parabola for focusing (i.e., 12 gratings grouped in four TGA's). This model simulates the influence of misalignment on all four TGA's of a compressor taking into account the measured wavefronts of the grating tiles. The performance of a tiled-grating compressor is fundamentally determined by the initial tiling performance and the long-term stability of a TGA. The initial tiling is constrained by the interferometric measurement, which is subject to disturbance caused by turbulence and vibration; the long-term stability of a TGA is determined by environmental stability, such as temperature and vibration. Taking into account the sensitivity of the tiling interferometer and the mechanical and environmental stabil-

ity of a TGA, the best-achievable tiling accuracy for each tile of each TGA was determined to be approximately ±0.2 μrad, ±0.2 μrad, and ±0.13 μm for tilt plus groove spacing change, tip plus IPR, and piston plus lateral shift, respectively. For each OMEGA EP compressor, there are eight outboard tiles to be aligned to their corresponding central tiles. Since there are three independent tiling parameters for each tile, the total number of independent tiling parameters is 24. It is necessary to understand and predict the combined effect of the tiling errors described above on the focal spot of the tiled-grating compressor. For each outboard tile of a TGA of the compressor, the tilt, tip, and piston were chosen as the independent tiling parameters to perform a Monte Carlo tolerance analysis, i.e., each outboard tile's position in terms of tilt, tip, and piston was randomly perturbed within the tiling accuracy. This simulation was done in the case of a flat grating-tile wavefront and a measured non-flat grating-tile wavefront. For both cases, the input beam of the compressor was flat. The mean and standard deviation values of the radius of 80% encircled energy, R_{80}, and Strehl ratio were calculated for 500 runs. Figure 115.2 shows the histograms of the far-field performance of 500 randomly realized tiled-grating compressors with a tiling accuracy tilt/ tip = ±0.2 μrad and piston = 0.13 μm for the grating tiles with a flat wavefront. The mean and standard deviation of R_{80} are 4.2 μm and 0.66 μm, respectively.

The size of each of the 12 holographically recorded MLD diffraction-grating tiles is 0.47 m × 0.43 m. The state-of-the-art wavefront quality for this size of grating tile is approximately 0.25 λ (peak-to-valley), λ (wavelength) = 1053 nm. Grating wavefront error consists of a substrate mirror term due to coat-
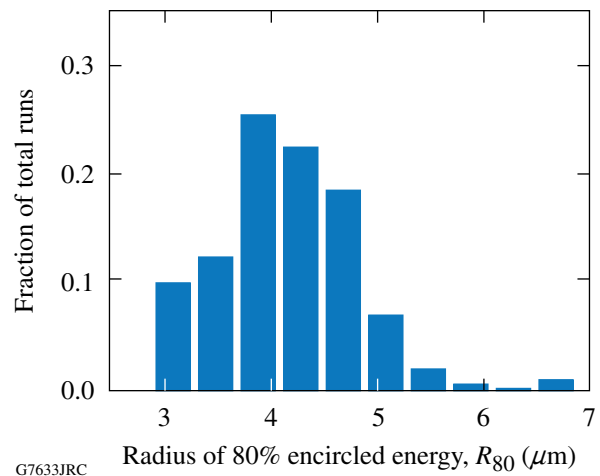

G7633JRC

Figure 115.2
The histograms of R_{80} for 500 simulations considering the experimental tiling error and flat grating-tile wavefront.

ing and a holographic term, which could add or cancel each other, depending on the orientation of the grating relative to the beam. The final wavefront of the compressor varies with the choice, order, and orientation of each of its 12 gratings. These properties were optimized to minimize the overall wavefront of the compressor using a matrix-based procedure that considers the measured wavefront of each individual grating tile at both orientations. We have modeled the focal-spot degradation caused by the static wavefront of all grating tiles for various compressor configurations. In these simulations, the three glass substrates of each TGA are perfectly aligned, i.e., there is no tiling error. The compressor configurations producing the minimum total wavefront error were selected for actual construction. Figure 115.3(a) shows the minimized wavefront map of one realization. The peak-to-valley and rms wavefront are 0.73 λ and 0.07 λ, respectively. The corresponding R_{80} is 7.3 μm. The design baseline corresponding to a flat wavefront is 2.6 μm. A Monte Carlo tiling-tolerance analysis predicted the focal-spot degradation under imperfect tiling conditions by using the measured wavefront of the tiles and the experimental tiling accuracy of tilt/tip ± 0.2 μrad and piston ± 0.13 μm. Figure 115.3(b) shows the histogram of R_{80} for 500 simulations. The mean and standard deviation of R_{80} are 7.7 μm and 0.8 μm, respectively. Considering the focal-spot size without tiling error (R_{80} = 7.3 μm) and the design baseline (R_{80} = 2.6 μm), we conclude that the focal-spot degradation is dominated by the static grating wavefront when submicroradian tiling accuracy can be achieved. We can also conclude that, given the same tiling accuracy, the focal-spot degradation caused by tiling error is greater for a compressor consisting of grating tiles with flat wavefront (R_{80} changes from 2.6 μm to 4.2 μm) than for that consisting of grating tiles with non-flat wavefront (R_{80} changes from 7.3 μm to 7.7 μm).
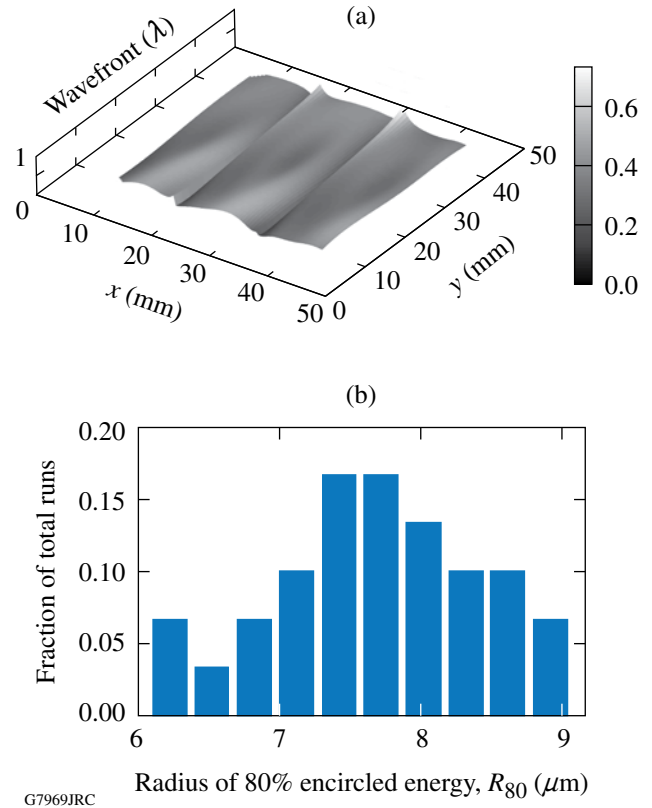

Figure 115.3
(a) The wavefront map of one compressor realization when there is no tiling error. (b) The histogram of R_{80} for 500 simulations when tiling error and grating-tile wavefront are taken into account.

Interferometric Tiling Technique in a Grating Compressor Chamber at Vacuum and the Performance of the Tiled TGA's

A 12-in.-aperture Fizeau interferometer was built for each compressor inside the grating compressor chamber (GCC) to tile individual TGA's at vacuum. The laser wavelength of the interferometer is 1053 nm. As shown in Fig. 115.4, the col-
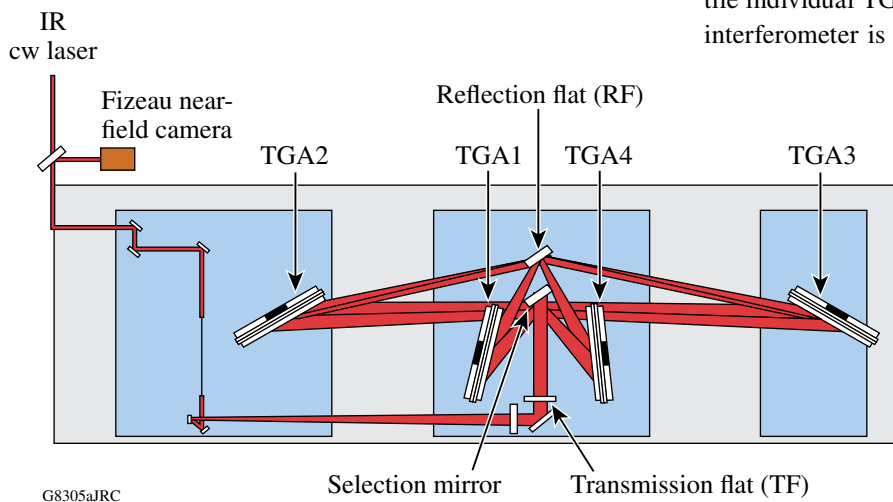

Figure 115.4
Optical layout for tiling each individual TGA with a Fizeau interferometer inside the GCC. The combined movement of the TGA selection mirror and RF makes it possible for the interferometer to see all of the gaps of the four TGA's, sequentially.

limated Fizeau beam is transmitted through the transmission flat and directed to two adjacent tiles of each one of the four TGA's by the selection mirror. The reflection flat (RF) is oriented to retroreflect the diffracted beam from each TGA at its working angle. Unique orientations of the TGA's, the selection mirror, and the RF were required to sequentially tile each of the eight gaps of four TGA's. The Fourier analysis of the resulting interferogram[9] was used to retrieve the phase of each tile and to calculate the differential tilt, tip, and piston between the central tile and an outboard tile. The differential values were used as feedback to control the tiling actuators to minimize the overall wavefront of the full TGA. This near-field tiling process has been automated.

To predict the focal-spot performance of a tiled-grating compressor, it is essential to obtain the overall wavefront and stability of a tiled TGA having three tiles. Before the TGA's were installed inside the GCC, a 24-in.-aperture Fizeau interferometer was used to tile each TGA and obtain the overall wavefront using an automated near-field method in a large-optics test facility.

Figures 115.5(a)–115.5(c) illustrate the automatic tiling process and show the phase map of the two tiles under alignment before, during, and at the end of the automatic tiling process, respectively. Minimized wavefront (rms wavefront = $0.0562\ \lambda$) of the two tiles was achieved after removing the angular and piston misalignment between the two tiles.

Figure 115.6(a) shows the overall rms wavefront of all tiled TGA's, which is under $0.08\ \lambda$. Figure 115.6(b) illustrates the typical tiling stability. The tiled wavefront of one of the eight TGA's was maintained below $0.09\ \lambda$ for at least 12 h by tiling actuators in a closed control loop. The stability test was done during the night since there were many other integration activities around the interferometer area during the day. Please note: the grating compressor vacuum chamber provides a much more controlled environment.

After all of the eight TGA's were installed inside the GCC, they were retiled using the GCC interferometers. The differential angle between two adjacent tiles was measured for 12 h by the Fizeau interferometer. Figure 115.7 shows the typical
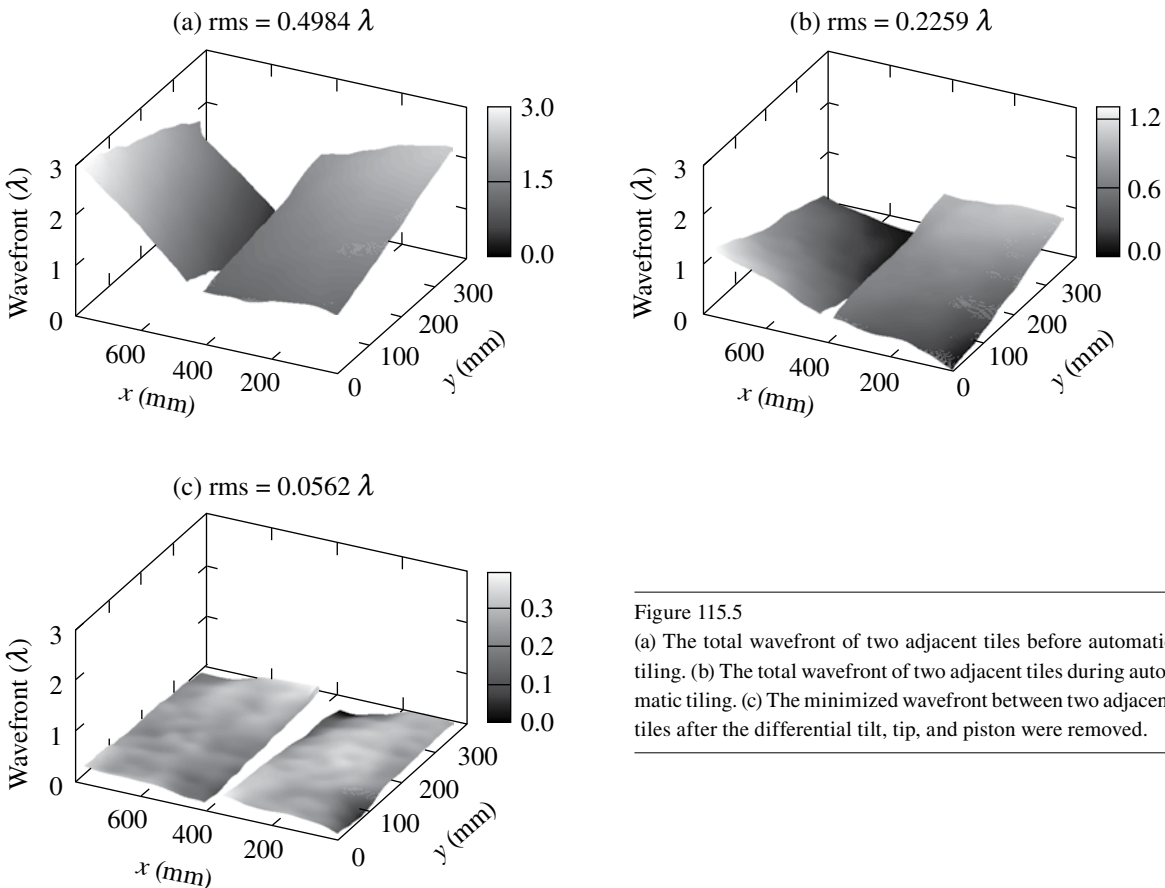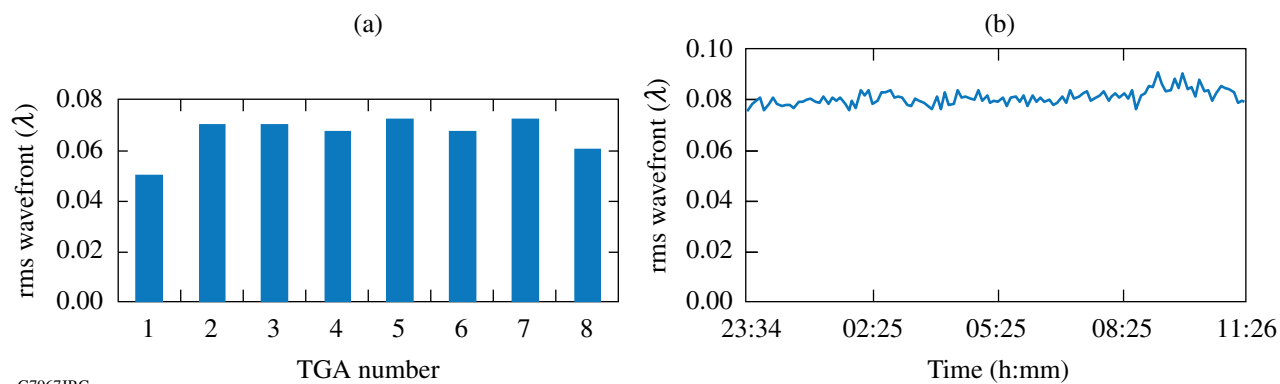

Figure 115.5
(a) The total wavefront of two adjacent tiles before automatic tiling. (b) The total wavefront of two adjacent tiles during automatic tiling. (c) The minimized wavefront between two adjacent tiles after the differential tilt, tip, and piston were removed.
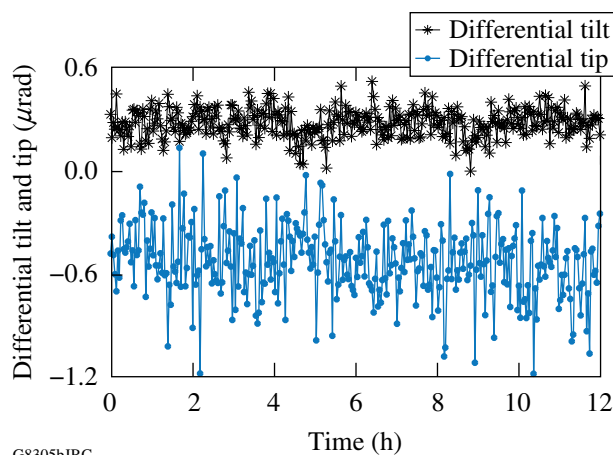
E17011JR

(a)

(b)

G7967JRC

Figure 115.6
(a) Root-mean-square (rms) tiled wavefronts of all eight TGA's; (b) typical wavefront stability of a tiled TGA.

G8305bJRC

Figure 115.7
Angular tiling stability in the GCC at vacuum.

angular tiling stability in the GCC at vacuum. The standard deviation of the differential tilt (horizontal) and differential tip (vertical) is 0.1 μrad and 0.2 μrad, respectively.

Performance Characterization and Optimization of Tiled-Grating Compressors

After individual TGA tiling, the four TGA's were rotated to their previously aligned compressor position. Any residual tiling misalignment among the four outboard tiles (i.e., one tile per TGA) on the same side of the beam can be canceled using one of the tiles (see the highlighted tiles in Fig. 115.8). We chose to use the outboard tiles of TGA4 to compensate the cumulative tiling error. This was done by a far-field analysis. A tiling apodizer array with three different apertures was placed in the collimated tiling-beam space. The translation of the tiling-apodizer array limited the illumination of the compressor to one single tile, two adjacent tiles, or all three tiles at a time. The far-field pattern of two adjacent tiles is compared to that of the central tiles in order

to obtain angular misalignment and differential phase information, therefore providing feedback to drive the corresponding tiling actuators of TGA4 to remove the residual tiling error. After this tiling optimization, the three-tile apodizer is translated into the beam to evaluate the final tiling performance.

It is not possible to directly compare the focal-spot performance of the tiled-grating compressor having four sets of TGA's (a total of 12 tiles) to that of a compressor consisting of four monolithic gratings with the same aperture size due to the unavailability of the latter. To evaluate the effect of tiling on focal-spot degradation, we apodized the beam size along the tiling (horizontal) direction to construct a sub-aperture compressor consisting of only the four central tiles. The aperture-size ratio between the single-central-tile compressor and the triple-tile compressor is 1:2.95 and 1:1 along the horizontal and vertical directions, respectively. Since the two compressors have the same beam size along the vertical direction, the two vertical lineouts were compared to evaluate focal-spot degradation due to tiling. The two horizontal lineouts were compared to show the aperture ratio between the two configurations. Figures 115.9(a) and 115.9(b) show the focal spots of the single-central-tile compressor and the triple-tile compressor, respectively. Figure 115.9(c) shows a comparison between two horizontal and vertical lineouts. In these plots, f_x and f_y are the dimensions, in microradians, of the focal spot along the horizontal and vertical directions.

The full width at half maximum (FWHM) of the focal-spot lineout ratio between the single-central-tile sub-aperture compressor and the triple-tile full-aperture compressor is 3:1 and 1:1 for the horizontal and vertical directions, respectively. This is expected when comparing a sub-aperture compressor to a properly aligned full-aperture grating compressor with four monolithic gratings. The profiles of two vertical lineouts are comparable. We can conclude that tiling does not degrade the

spatial performance of the tiled-grating compressor. A triple-tile compressor delivers a tighter focal spot and three times the energy of a single-central-tile-only compressor.

After compressor alignment and grating tiling, temporal compression was optimized by changing the dispersion of the stretcher. The optical parametric chirped-pulse–amplification
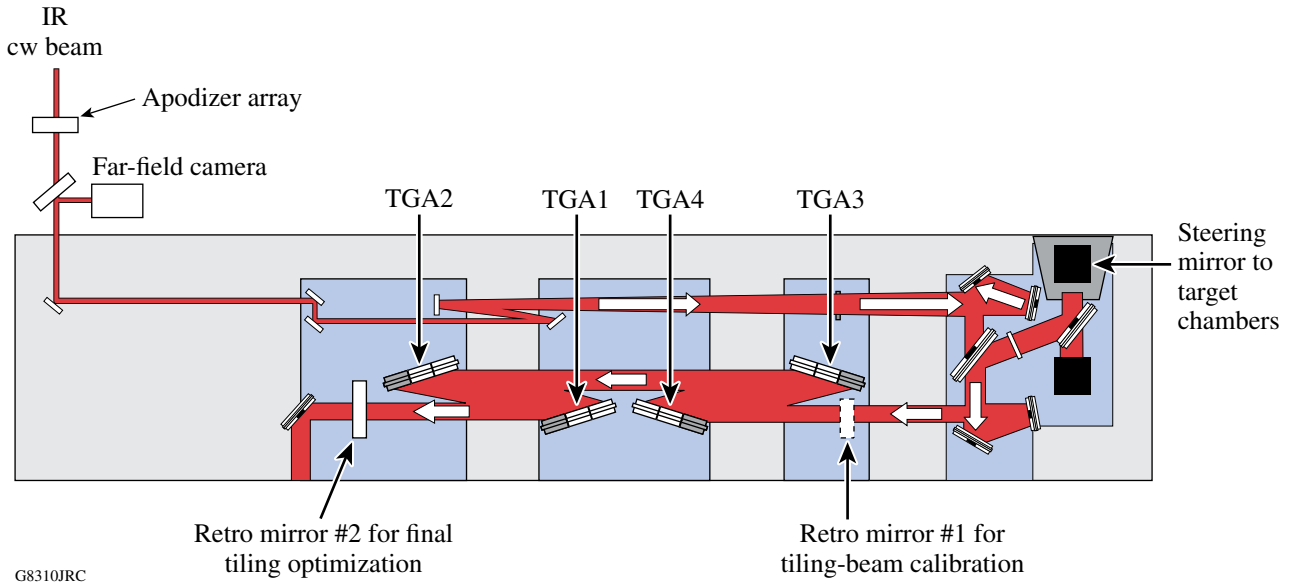

Figure 115.8
Optical layout for evaluating and optimizing overall tiling performance of the whole compressor. Before tiling optimization, retro mirror #1 was used to calibrate the far field of the tiling beam. During tiling optimization, this mirror was removed from the beam. The tiling beam went through the compressor and was reflected back by retro mirror #2. One of the four highlighted tiles was chosen to optimize the overall tiling performance.
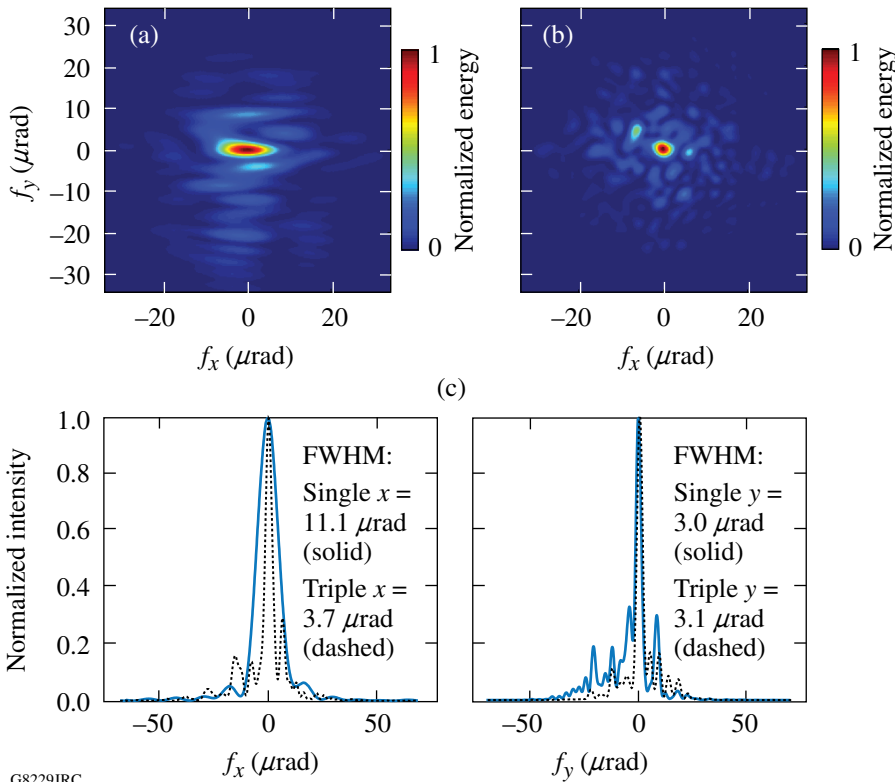

Figure 115.9
(a) Focal spot of the single-central-tile compressor; (b) focal spot of the triple-tile compressor; (c) comparison between the horizontal lineouts and vertical lineouts of the two focal spots.

(OPCPA) front end is operated at 5 Hz (Ref. 10). The autocorrelation of the output pulses was measured for both single-central-tile and triple-tile configurations for both OMEGA EP compressors. Figures 115.10(a) and 115.10(b) show the measured autocorrelations with a decorrelation factor of 1.34 (calculated from the measured spectrums). The pulse width is 630 fs for both the single-central-tile and triple-tile configurations of compressor 1. Similarly, we obtained a 600-fs pulse width for the single-central-tile and triple-tile configurations of compressor 2. The transform-limited pulse width is 400 fs and 410 fs for compressors 1 and 2, respectively. Single- and triple-tile configurations delivered the same pulse width. Therefore, there is no change in pulse duration due to tiling.
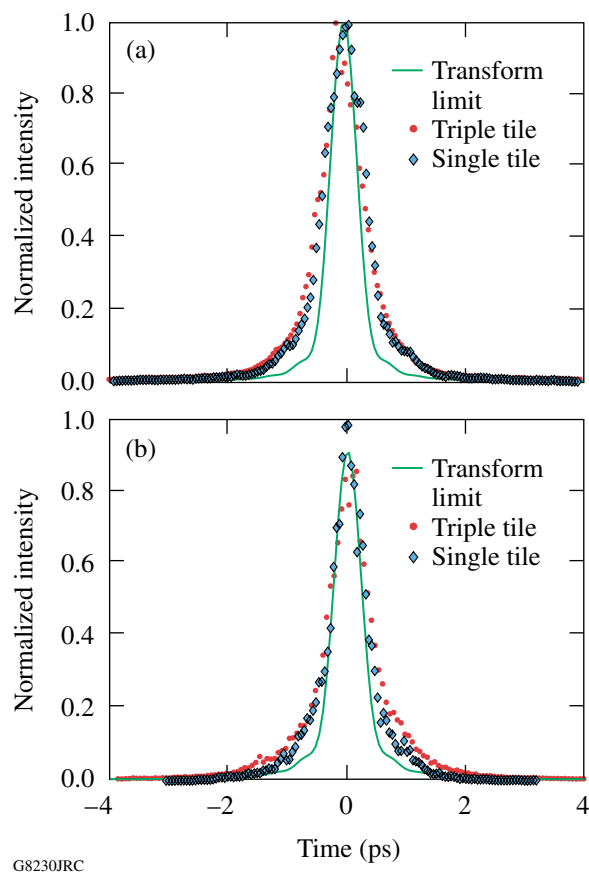

Figure 115.10
(a), (b) Autocorrelation scanning results for single-tile and triple-tile configurations for (a) compressor 1 and (b) compressor 2.

Conclusions

In conclusion, we have developed and built eight precision tiled-grating assemblies. Submicroradian tiling accuracy and stability have been achieved for all eight TGA's. A ray-tracing

model predicts that the static wavefront of the grating tiles dominates focal-spot degradations when submicroradian tiling accuracy is achieved. For the first time, we demonstrated pulse compression in two 1.5-m, large-aperture tiled-grating compressors for the OMEGA EP high-energy, petawatt-class laser system. Measurement of the tiled-grating compressors verified the model prediction and confirmed that the focal-spot degradation caused by tiling is minimal. Output-pulse autocorrelation measurements verified that both compressors achieved subpicosecond pulse widths and there is no pulse duration change due to tiling. This demonstration opens the path for constructing even larger tiled-grating compressors (multiple meters) for high-energy, high-power OPCPA systems.

REFERENCES

1. J. H. Kelly, L. J. Waxer, V. Bagnoud, I. A. Begishev, J. Bromage, B. E. Kruschwitz, T. J. Kessler, S. J. Loucks, D. N. Maywar, R. L. McCrory, D. D. Meyerhofer, S. F. B. Morse, J. B. Oliver, A. L. Rigatti, A. W. Schmid, C. Stoeckl, S. Dalton, L. Folnsbee, M. J. Guardalben, R. Jungquist, J. Puth, M. J. Shoup III, D. Weiner, and J. D. Zuegel, J. Phys. IV France **133**, 75 (2006).

2. J. A. Britten *et al.*, in *Laser-Induced Damage in Optical Materials: 2003*, edited by G. J. Exarhos *et al.* (SPIE, Bellingham, WA, 2004), Vol. 5273, pp. 1–7.

3. T. Zhang, M. Yonemura, and Y. Kato, Opt. Commun. **145**, 367 (1998).

4. Y. Zuo *et al.*, Opt. Lett. **32**, 280 (2007).

5. T. J. Kessler, J. Bunkenburg, H. Huang, A. Kozlov, and D. D. Meyerhofer, Opt. Lett. **29**, 635 (2004).

6. A. Cotel *et al.*, Opt. Express **15**, 2742 (2007).

7. J. Qiao, A. Kalb, M. J. Guardalben, G. King, D. Canning, and J. H. Kelly, Opt. Express **15**, 9562 (2007).

8. *LLE Review Quarterly Report* **100**, 242, Laboratory for Laser Energetics, University of Rochester, Rochester, NY, LLE Document No. DOE/SF/19460-578, NTIS Order No. PB2006-106672 (2004). (Copies may be obtained from the National Technical Information Service, Springfield, VA 22161.)

9. M. Takeda, H. Ina, and S. Kobayashi, J. Opt. Soc. Am. **72**, 156 (1982).

10. V. Bagnoud, I. A. Begishev, M. J. Guardalben, J. Puth, and J. D. Zuegel, Opt. Lett. **30**, 1843 (2005).